Journal of Organometallic Chemistry 891 (2019) 20–27

Contents lists available at ScienceDirect

Journal of Organometallic Chemistry

journal homepage: www.elsevier.com/locate/jorganchem

Synthesis, photophysical and electrochemical properties of naphthaldimine based boron complexes☆

Ramu V. Ranga Naidu Chinta, Basava Punna Rao Aradhyula, Anna Chandrasekar Murali, Krishnan Venkatasubbaiah*

School of Chemical Sciences, National Institute of Science Education and Research (NISER), HBNI, Bhubaneswar, 752050, Odisha India

ARTICLE INFO

Article history:
Received 24 January 2019
Received in revised form
16 March 2019
Accepted 10 April 2019
Available online 14 April 2019

Keywords:
Tetra-coordinated boron
Diboron
Triboron
N,O-chelated boron
Imino boron

ABSTRACT

Naphthaldehyde based imine ligands (**L1H$_2$** and **L2H$_3$**) have been designed and synthesized. The coordination of imine ligands with BF_2 motif and BPh_2 motif lead to the formation of complexes **1**–**4**. Both the ligands and the boron complexes were characterized by multinuclear NMR spectroscopy and mass spectrometry. Boron NMR of the complexes revealed that the boron atom is in tetracoordinate environment. The optical properties of the complexes and the ligands in solution suggest that borylation enhanced the quantum yields of the ligands. The electrochemical studies indicated that diboron complexes (**1** & **3**) and triboron complexes (**2** & **4**) exhibit two and three separate reduction waves respectively.

1. Introduction

Innovative organic luminescent fluorophores [1,2] have attracted much attention due to their numerable applications in biological as well as in optoelectronic devices [3–12]. Incorporation of main-group elements into the framework of organic fluorophores has provided a new opportunity to tune the optical properties of the fluorophores. Among the many main-group incorporated fluorophores, boron-based fluorophores such as boron-dipyrromethene (BODIPY) [13–16] as well as N∩O [17–28]; N∩N [29–35] and N∩C [36,37] chelates have gained much interest due to the their attractive photo physical properties. Of these extended π-conjugated systems, the N∩O chelated boron system 'boranils' were derived from the salicylaldimine {aniline-imine (anil)} ligands [38–43]. The 'anils' were known for extremely complex behavior involving ultrafast excited state intramolecular proton transfer (ESIPT), torsional dynamics, photochromism, thermochromism, and solvatochromism [44–53].

It has been demonstrated that multiboron compounds not only increase the electron-accepting capabilities but also enhance the fluorescence quantum yields [42,43]. Having this in mind, recently, we have reported N∩O chelated diboron complexes (boranils) [54,55] where they show tunable absorption and emission properties and moderate quantum yields in solution. In pursuit of new multiboron complexes with improved photophysical properties, prompted us to prepare naphthaldimine based boron complexes. Herein, we describe the synthesis, optical and electrochemical properties of novel tetra-coordinate di- and triboron complexes.

2. Experimental

2.1. General procedures

Reagents were used as received unless otherwise noted. THF and toluene were distilled from Na/benzophenone prior to use. Chlorinated solvents were distilled from CaH_2. The starting material 6-hexyl-2-hydroxy-1-naphthaldehyde was prepared by using literature reports [56,57]. NMR spectra were recorded on Bruker 700 and ARX 400 spectrometers at room temperature. All ^{1}H (700 MHz), ^{13}C (176 MHz), ^{1}H (400 MHz) and ^{13}C (100 MHz) NMR spectra were referenced internally to solvent signals. ^{11}B NMR spectra were referenced externally to $BF_3{\cdot}OEt_2$ in $CDCl_3$ ($\delta = 0$ ppm), and ^{19}F NMR spectra were referenced to α,α,α-trifluorotoluene (0.05% in $CDCl_3$; $\delta = -63.73$ ppm). ESI mass spectra were recorded with a

☆ Dedicated to Professor V. Chandrasekhar on the occasion of his 60th birthday.
* Corresponding author.
E-mail address: krishv@niser.ac.in (K. Venkatasubbaiah).

https://doi.org/10.1016/j.jorganchem.2019.04.008
0022-328X/

Bruker microTOF-QII mass spectrometer. The absorbance spectra were recorded with a Perkin–Elmer Lambda 750 UV/Visible spectrometer. The fluorescence spectra were recorded with a Perkin–Elmer LS-55 Fluorescence Spectrometer and corrected for the instrumental response. Absolute fluorescence quantum yields in solution and solid state were measured by integrating sphere method using Edinburgh FS5 spectrofluorometer. Electrochemical measurements were performed with a conventional three-electrode cell and an electrochemical workstation (CH Instrument 1100A). The three-electrode system consisted of a glassy carbon working electrode, a Pt wire as the secondary electrode, and a Ag wire as the reference electrode. The voltammograms were recorded with ca. 1.0×10^{-3} M solutions in DME containing $Bu_4N(PF_6)$ (0.1 M) as the supporting electrolyte. The scans were referenced after the addition of a small amount of ferrocene as the internal standard. Single crystal X-ray diffraction data were collected on Bruker APEX-II CCD diffractometer using Mo-Kα radiation (0.71073 Å). Structure solution by direct methods was achieved through the use of the SHELXT program, and the structural model refined by full-matrix least-squares on F^2 using SHELXL [58] by using the Olex2 software. The non-hydrogen atoms were refined with anisotropic thermal parameters except severely disordered hexyl moiety. Hydrogen atoms (except for one of the hexyl group) were placed using idealized geometric positions (with free rotation for methyl groups), allowed to move in a "riding model" along with the atoms to which they were attached, and refined isotropically. CCDC-1893,211 contain the supplementary crystallographic data for this paper. These data can be obtained free of charge from The Cambridge Crystallographic Data Centre *via* www.ccdc.cam.ac.uk/data_request/cif. DFT calculations were performed with the Gaussian09 program. The structures were optimized using 6-31G (B3LYP) as the basis set. In order to reduce the computation time, "Hexyl" on the naphthyl was replaced with "Me". The input files for **1** and **3** were generated using the X-ray data of compound **3**, whereas for **2** and **4** the input files were generated using Gauss-View. Excitation data were determined using TD-DFT (B3LYP) calculations.

2.2. General procedure for the synthesis of ligands (*L1H₂* and *L2H₃*)

The precursor (aldehyde) for the ligands **L1H₂** and **L2H₃** *i.e.*, 6-hexyl-2-hydroxy-1-naphthaldehyde was synthesized by following the literature reported procedure [56,57]. Ethanol (50 mL) was added to a 250 mL round-bottomed flask containing 6-hexyl-2-hydroxy-1-naphtaldehyde and 1,4-phenylene diamine for **L1H₂** or 1,3,5-triamino benzene for ligand **L2H₃** [59]. To the reaction mixture few drops of glacial acetic acid was added. The resultant yellow mixture was stirred for overnight at reflux condition. Over the period of the time the reaction mixture yielded cloudy precipitates. These precipitates were filtered, washed with cold methanol and dried under vacuum.

2.2.1. Synthesis of ligand *L1H₂*

The quantities involved are as follows: 6-hexyl-2-hydroxy-1-naphtaldehyde (1.04 g, 4.07 mmol), 1,4-phenylene diamine (0.20 g, 1.85 mmol). Colour: Red; Yield: 1.01 g, (93%); mp: 212 °C; ^{1}H NMR (400 MHz, $CDCl_3$): δ 15.35 (s, 2H), 9.38 (s, 2H), 8.06 (d, $J = 8.0$ Hz, 2H), 7.77 (d, $J = 12.0$ Hz, 2H), 7.52 (s, 2H), 7.45 (s, 4H), 7.40 (d, $J = 8.0$ Hz, 2H), 7.10 (d, $J = 12.0$ Hz, 2H), 2.73 (t, $J = 8.0$ Hz, 4H), 1.76–1.63 (m, 4H), 1.35 (m, 13H), 0.90 (t, $J = 4.0$ Hz, 6H); ^{13}C NMR (101 MHz, $CDCl_3$): δ 168.43, 155.16, 144.55, 138.45, 136.40, 131.34, 129.54, 128.33, 127.82, 121.83, 121.65, 119.12, 109.32, 35.68, 31.91, 31.55, 29.16, 22.78, 14.26; HR-MS (ESI): calcd. for $C_{40}H_{44}N_2O_2$ ($[M+H]^+$): 585.3476, found: 585.3446.

2.2.2. Synthesis of ligand *L2H₃*

The quantities involved are as follows: 6-hexyl-2-hydroxy-1-naphtaldehyde (2.18 g, 8.5 mmol), 1,3,5-tri amino benzene (0.30 g, 2.43 mmol). Colour: Brown, Yield: 1.73 g, (85%); mp: 168 °C; ^{1}H NMR (400 MHz, $CDCl_3$) δ 15.16 (s, 3H), 9.46 (s, 3H), 8.11 (d, $J = 8.0$ Hz, 3H), 7.79 (d, $J = 8.0$ Hz, 3H), 7.52 (s, 3H), 7.41 (d, $J = 8.0$ Hz, 3H), 7.21 (s, 3H), 7.11 (d, $J = 8.0$ Hz, 3H), 2.73 (t, $J = 8.0$ Hz, 6H), 1.75–1.63 (m, 6H), 1.43–1.25 (m, 18H), 0.89 (t, $J = 8.0$ Hz, 9H); ^{13}C NMR (101 MHz, $CDCl_3$) δ 168.36, 156.63, 148.97, 138.68, 136.86, 131.33, 129.75, 128.31, 127.89, 121.44, 119.35, 110.43, 109.35, 35.67, 31.90, 31.54, 29.16, 22.79, 14.26; HR-MS (ESI): calcd. for $C_{57}H_{63}N_3O_3$ ($[M+Na]^+$): 860.4762, found: 860.4767.

2.2.3. Synthesis and characterization of difluoro boron complexes

Tetrahydrofuran (20 mL) was added to a 50 mL round-bottomed flask containing ligand (**L1H₂** or **L2H₃**) and NaH under nitrogen atmosphere at 0 °C. The reaction mixture was warmed to ambient temperature and stirred at that temperature for 2 h. The reaction mixture was then cooled to 0 °C; and $BF_3{\cdot}OEt_2$ was added dropwise and the mixture was stirred for 24 h. The reaction mixture was filtered through Celite, and the resultant filtrate was concentrated to yield a pale yellow solid, which was purified by recrystallization in diethyl ether.

2.2.4. Complex *1*

The quantities involved are as follows: **L1H₂** (0.20 g, 0.34 mmol), NaH (0.02 g, 0.85 mmol), $BF_3{\cdot}OEt_2$ (0.86 mL, 6.82 mmol). Yield: 0.20 g, (85%); mp: 249 °C; ^{1}H NMR (400 MHz, $CDCl_3$): δ 9.15 (s, 2H), 8.10 (d, $J = 12.0$ Hz, 2H), 8.01 (d, $J = 8.0$ Hz, 2H), 7.76 (s, 4H), 7.64 (s, 2H), 7.55 (d, $J = 8.0$ Hz, 2H), 7.28 (s, 1H), 7.26 (s, 1H), 2.79 (t, $J = 8.0$ Hz, 4H), 1.78–1.64 (m, 4H), 1.48–1.23 (m, 12H), 0.91 (t, $J = 8.0$ Hz, 6H); ^{13}C NMR (176 MHz, $CDCl_3$): δ 162.88, 158.54, 143.18, 141.81, 140.46, 131.34, 129.73, 128.70, 128.48, 125.24, 120.38, 119.31, 109.02, 35.71, 31.85, 31.45, 29.10, 22.75, 14.24; ^{11}B NMR (128 MHz, $CDCl_3$): δ 0.95; ^{19}F NMR (377 MHz, $CDCl_3$): δ −134.0 (d, $J = 26.4$ Hz); IR (KBr): $\bar{\nu}$ = 2926 (m), 2855 (m), 1609 (s), 1557 (s), 1503 (s), 1467 (s), 1409 (s), 1386 (s), 1355 (s), 1309 (s); HR-MS (ESI): calcd. for $C_{40}H_{42}B_2F_4N_2O_2$ ($[M+Na]^+$): 703.3274, found: 703.3270.

2.2.5. Complex *2*

The quantities involved are as follows: **L2H₃** (0.30 g, 0.30 mmol), NaH (0.03 g, 1.25 mmol), $BF_3{\cdot}OEt_2$ (1.35 mL, 10.74 mmol). Yield: 0.30 g, (85%); mp: 258 °C; ^{1}H NMR (700 MHz, $CDCl_3$): δ 9.24 (s, 3H), 8.11 (d, $J = 9.1$ Hz, 3H), 8.03 (d, $J = 8.5$ Hz, 3H), 7.96 (s, 3H), 7.62 (s, 3H), 7.55 (d, $J = 8.4$ Hz, 3H), 7.27 (s, 2H), 7.25 (s, 1H), 2.77 (t, $J = 4.0$ Hz, 6H), 1.74–1.65 (m, 6H), 1.40–1.21 (m, 18H), 0.89 (t, $J = 8.0$ Hz, 9H); ^{13}C NMR (101 MHz, $CDCl_3$): δ 163.39, 159.31, 144.89, 142.58, 140.66, 131.64, 129.70, 128.66, 128.45, 120.20, 119.59, 119.46, 109.16, 35.67, 31.84, 31.37, 29.09, 22.75, 14.23; ^{11}B NMR (128 MHz, $CDCl_3$): δ 0.97; ^{19}F NMR (377 MHz, $CDCl_3$): δ −133.1 (d, $J = 22.6$ Hz); IR (KBr): $\bar{\nu}$ = 2927 (m), 2854 (m), 1614 (s), 1600 (s), 1553 (s), 1466 (s), 1413 (s), 1388 (s), 1355 (s), 1311 (s); HR-MS (ESI): calcd. for $C_{57}H_{60}B_3N_3F_6O_3$ ($[M+Na]^+$): 1004.4735, found: 1004.4712.

2.2.6. Synthesis and characterization of diphenyl boron complexes

Ligand (**L1H₂** or **L2H₃**) was taken in a sealed tube to that triphenylborane was added under nitrogen atmosphere followed by dry toluene (5 mL). The reaction mixture was refluxed for 12 h under nitrogen atmosphere. The reaction mixture was cooled and the solvent was evaporated by vacuum distillation leaving behind a glassy residue. To the resultant residue dry *n*-hexane (5 ml) was added under nitrogen atmosphere and the mixture was heated with vigorous stirring for 30 min. After cooling to room temperature, the solvent was decanted off the insoluble precipitate was

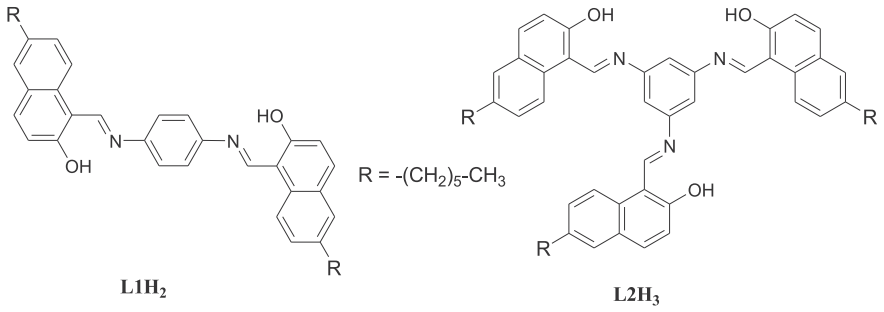

Fig. 1. Ligands used in the present study.

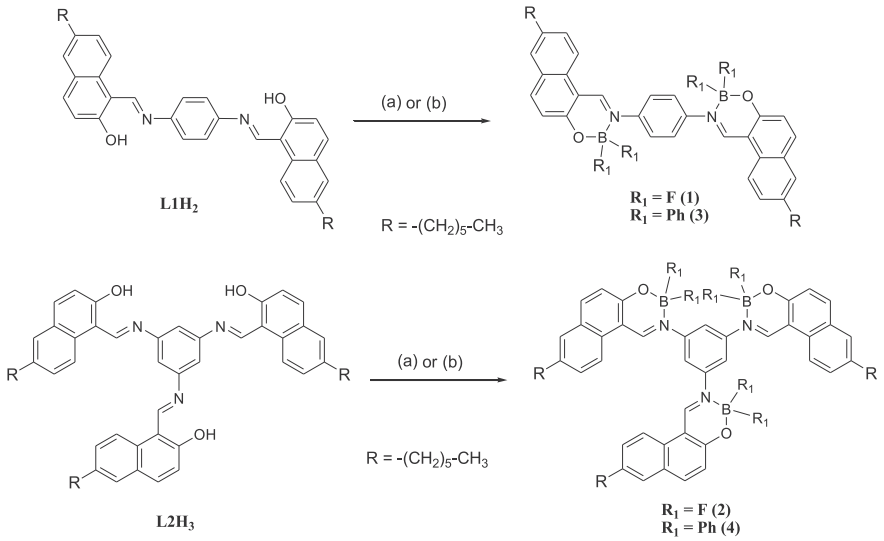

Scheme 1. Synthesis of boron complexes **1**–**4**. (a) NaH, $BF_3.OEt_2$, THF (for **1** & **2**); (b) $B(C_6H_5)_3$, toluene (for **3** & **4**).

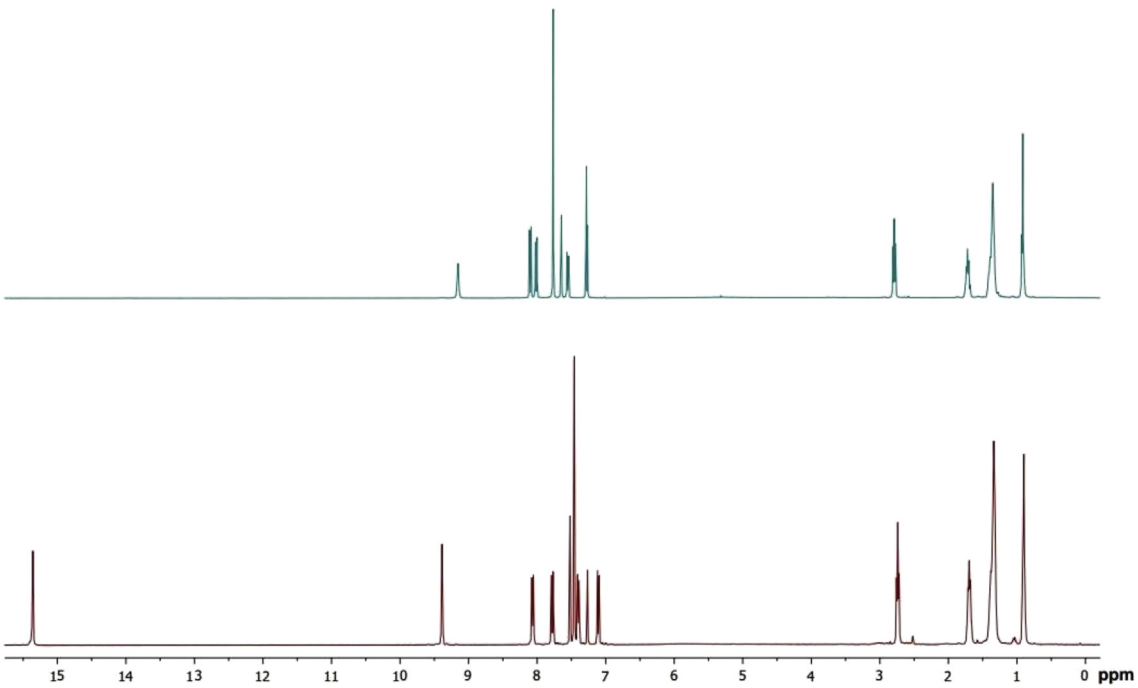

Fig. 2. Comparison of phenolic proton and observable shift in peak position of aromatic protons form the Stacked ^1H NMR spectrum of the ligand **L1H$_2$** (bottom) and its difluoro boron complex **1** (top).

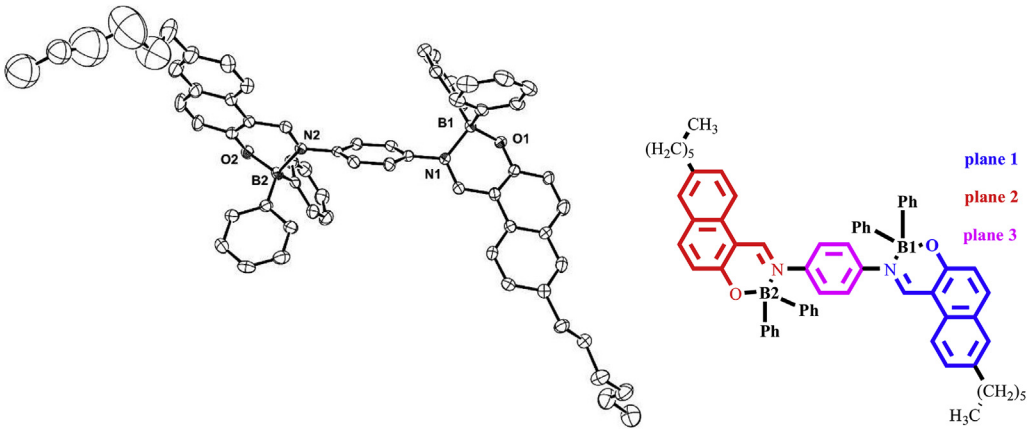

Fig. 3. Solid state structure of the complex **3**, hydrogen atoms omitted for the clarity (left); chemdraw structure of complex **3** (right). Selected bond lengths (Å) bond angles (°) are as follows: B1–N1:1.637(4), B1–O1: 1.494(4), B1–C1: 1.619(5), B1–C7: 1.604(5), B2–N2:1.635(4), B2–O2: 1.493(4), B2–C42: 1.614(5), B2–C36: 1.621(5), O1–B1–N1: 104.0(2), O1–B1–C7: 106.9(3), O1–B1–C1: 109.9(3), C7–B1–N1: 112.4(2), C1–B1–N1: 107.2(2), C7–B1–C1: 115.7(3), O2–B2–N2: 103.9(3), O2–B2–C42: 106.8(3), O2–B2–C36: 111.0(3), C42–B2–N2: 112.3(3), C36–B2–N2: 106.8(2), C42–B2–C36: 115.4(3).

dried under vacuum. Crystallization was done using CH_2Cl_2/*n*-hexane mixture.

2.2.7. Complex **3**

The quantities involved are as follows: **L1H$_2$** (0.20 g, 0.34 mmol), triphenylborane (0.21 g, 0.85 mmol). Yield: 0.29 g, (93%); mp: 219 °C; ^{1}H NMR (400 MHz, $CDCl_3$): δ 8.81 (s, 2H), 7.87 (d, J = 8.0 Hz, 2H), 7.78 (d, J = 8.0 Hz, 2H), 7.49 (s, 2H), 7.39 (d, J = 8.0 Hz, 10H), 7.16 (dd, J = 4.0, 12.0 Hz, 14H), 6.95 (s, 4H), 2.71 (t, J = 8.0 Hz, 4H), 1.65 (m, 4H), 1.32–1.27 (m, 12H), 0.89 (t, J = 8.0 Hz, 6H); ^{13}C NMR (101 MHz, $CDCl_3$): δ 165.22, 157.49, 145.41, 140.69, 139.33, 133.78, 130.54, 130.52, 128.53, 128.01, 127.18, 126.64, 125.18, 121.48, 119.24, 111.48, 35.69, 31.86, 31.54, 29.07, 22.75, 14.24; ^{11}B NMR (128 MHz, $CDCl_3$): δ 5.19; IR (KBr): $\bar{\nu}$ = 2925 (m), 2853 (m), 1607 (s), 1550 (s), 1498 (s), 1459 (s), 1431 (s), 1403 (s), 1385 (s), 1347 (s); HR-MS (ESI): calcd. for $C_{64}H_{62}B_2N_2O_2$ ($[M+Na]^+$): 935.4909, found: 935.4930.

2.2.8. Complex **4**

The quantities involved are as follows: **L2H$_3$** (0.30 g, 0.36 mmol), triphenylborane (0.32 g, 1.32 mmol). Yield: 0.45 g, (93%); mp: 137 °C; ^{1}H NMR (700 MHz, $CDCl_3$): δ 8.26 (d, J = 7.7 Hz, 2H), 8.12 (s, 2H), 7.86 (d, J = 9.1 Hz, 2H), 7.68 (d, J = 9.1 Hz, 2H), 7.61 (t, J = 7.7 Hz, 2H), 7.52 (t, J = 7.7 Hz, 2H), 7.48–7.46 (m, 5H), 7.29 (d, J = 9.1 Hz, 9H), 7.21–7.17 (m, 15H), 7.08 (d, J = 9.1 Hz, 3H), 6.77 (s, 2H), 2.74 (t, J = 7.7 Hz, 6H), 1.70–1.66 (m, 6H), 1.39–1.32 (m, 18H), 0.90 (d, J = 7.0 Hz, 9H); ^{13}C NMR (176 MHz, $CDCl_3$): δ 165.62, 157.68, 146.12, 141.29, 139.64, 135.80, 133.78, 132.86, 130.30, 128.43, 128.15, 127.98, 127.43, 126.78, 121.29, 120.34, 120.23, 112.08, 35.72, 31.88, 31.60, 29.09, 22.77, 14.26; ^{11}B NMR (128 MHz, $CDCl_3$): δ −0.18; IR (KBr): $\bar{\nu}$ = 2924 (m), 2853 (m), 1609 (s), 1544 (s), 1513 (w), 1455 (s), 1431 (s), 1380 (s), 1345 (s), 1308 (s); HR-MS (ESI): calcd. for $C_{93}H_{90}B_3N_3O_3$ ($[M+Na]^+$): 1352.7164, found: 1352.7113.

Table 1
Photophysical data of imine ligands **L1H$_2$** and **L2H$_3$** and their complexes **1**–**4**.

Compound	Solvent	λ_{max}[a] (nm)	ε_{max} ($M^{-1}cm^{-1}$ x 10^3)	λ_{em}[a,b] (nm)	Φ_F[c] (%)	Stokes shift nm (cm^{-1})
L1H$_2$	Toluene	344, 423, 498[d]	12.9, 26.4, 07.3	546	<1	123 (5326)
	CH_2Cl_2	341, 428, 493[d]	14.7, 25.1, 15.1	546	<1	118 (5049)
	THF	341, 426, 497[d]	15.5, 29.6, 11.9	542	<1	116 (5024)
	CH_3CN	338, 428, 487[d]	15.2, 25.2, 17.2	539	<1	111 (4812)
L2H$_3$	Toluene	329, 397, 480[d]	33.1, 41.8, 08.5	507	<1	110 (5465)
	CH_2Cl_2	327, 396, 479[d]	34.8, 39.1, 16.5	511	<1	115 (5683)
	THF	326, 396, 477[d]	37.3, 43.3, 15.4	509	<1	113 (5606)
	CH_3CN	324, 396, 474[d]	36.1, 38.1, 21.7	507	<1	111 (5529)
Compound 1	Toluene	355, 436	18.1, 30.5	508	43	72 (3251)
	CH_2Cl_2	353, 430	22.6, 33.5	507	44	77 (3532)
	THF	349, 425	19.7, 29.1	505	35	80 (3727)
	CH_3CN	348, 422	21.7, 31.2	502	30	80 (3776)
Compound 2	Toluene	360, 433	26.4, 38.8	493	48	60 (2811)
	CH_2Cl_2	357, 428	30.6, 39.9	495	44	67 (3162)
	THF	347, 418	26.4, 33.5	490	26	72 (3515)
	CH_3CN	349, 419	28.5, 36.7	495	18	76 (3664)
Compound 3	Toluene	352, 462	17.9, 19.5	569	35	107 (4070)
	CH_2Cl_2	350, 459	20.2, 20.3	568	47	109 (4181)
	THF	346, 455	15.9, 16.5	568	32	113 (4372)
	CH_3CN	344, 452	19.5, 19.8	561	27	109 (4299)
Compound 4	Toluene	353, 453	23.1, 21.1	562	29	109 (4281)
	CH_2Cl_2	352, 450	23.4, 20.8	561	31	111 (4397)
	THF	348, 445	19.9, 17.4	560	21	115 (4615)
	CH_3CN	345, 440	23.3, 19.8	559	19	119 (4838)

[a] Absorption maximum (Concentration: 3.5 x 10^{-5} M).
[b] Excited at the absorption maximum.
[c] Fluorescence quantum yields were measure using an integrating sphere.
[d] Shoulder.

3. Results and discussion

The desired imine ligands (**L1H$_2$** and **L2H$_3$**) were synthesized in a one-step reaction by refluxing 1,4-phenylene diamine for **L1H$_2$** or 1,3,5-triamino benzene for **L2H$_3$** with 6-hexyl-2-hydroxy-1-naphthaldehyde [56] in absolute ethanol (Fig. 1). The boron precursors *i.e.*, $BF_3.OEt_2$ and BPh_3 were used to make the boron complexes using the ligands **L1H$_2$** and **L2H$_3$**. Addition of excess amount of $BF_3.OEt_2$ to the sodium phenoxide of the ligands in dry THF yielded the difluoroborane complexes **1** and **2**. While the reaction of triphenylborane ($(C_6H_5)_3B$) in dry toluene under reflux conditions yielded the diphenylborane complexes **3** and **4** (Scheme 1). Both the ligands (**L1H$_2$** and **L2H$_3$**) were characterized by ^1H and ^{13}C NMR spectroscopy and reflecting their molecular structure in each case. ^1H NMR spectra of the ligands have shown a singlet in the far downfield region (~15 ppm) which represents the H-bonded phenolic proton. A representative proton NMR spectra of ligand **L1H$_2$** and difluoro borane (**1**) are shown in Fig. 2. The number of carbon signals observed in the ^{13}C NMR spectrum is in well agreement with the proposed structure of the ligands. The borylated complexes were also characterized by various NMR spectroscopic techniques. Formation of the boron complexes have been readily assessed by the disappearance of the downfield singlet corresponding to the H-bonded phenolic proton in the ^1H NMR spectroscopy. In addition to the disappearance of the phenolic proton (Fig. 2), the shift in the peak position and the number of signals in the aromatic region with respect to aliphatic signals supports the chelation of ligand to the boron center. ^{19}F NMR exhibit poor-resolved quartet [60] at around -133 ppm for both the complexes. Boron NMR spectroscopy of all the complexes exhibit a peak at around 1.00 ppm which supports the tetracoordinate nature of the boron center.

All the compounds have also been characterized by infrared spectroscopy. The characteristic C=N imine stretching band was observed in the range of 1620–1630 cm^{-1} for all the complexes.

The formation of complex **3** was further analysed by single crystal X-ray analysis. The complex has been crystalized in a triclinic system with a space group $P\bar{1}$; the refinement data related to the same has been presented in Table S1. Molecular structure of the complex along with important bond lengths and bond angles are represented in Fig. 3. As shown in the figure, the boron centres adopts a distorted tetrahedral geometry with N,O chelation. The B–O and B–N bond lengths and C–N–B, C–O–B and N–B–O bond angles are amenable to the other literature reported tetracoordinate boron systems [61–63]. The boron atom coordinates to the nitrogen atom to form a strain free six membered ring. Both the boron atoms deviates by 0.57 (B1) Å and 0.59 (B2) Å from the plane defined by 'naphthyl' carbon atoms, oxygen, iminocarbon and nitrogen atoms (Fig. 3). The interplanar angles between plane 1 & plane 2 is 89.39 ° whereas plane 1 & plane 3 and plane 2 & plane 3 are 45.15 ° and 48.86 ° respectively (Fig. 3, chemdraw).

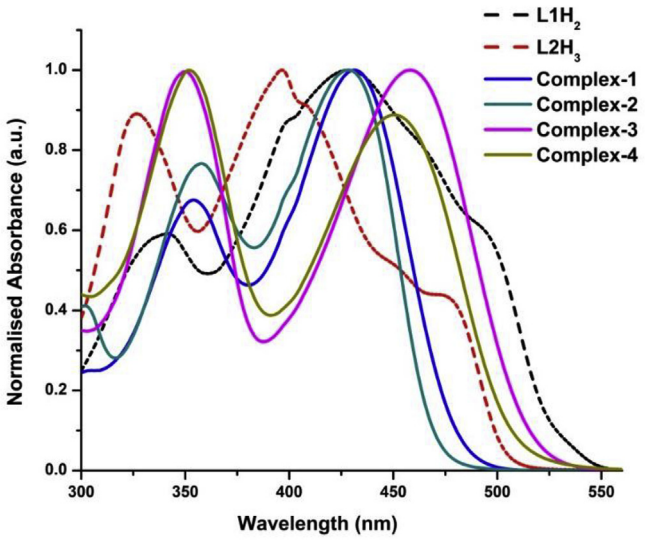

Fig. 4. Normalized absorbance spectra of the ligands and boron complexes at a concentration of 35 μM in CH_2Cl_2 solutions.

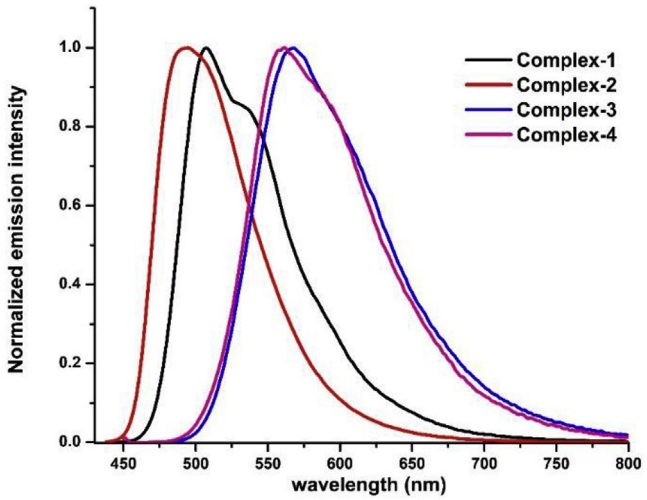

Fig. 5. Normalized fluorescence spectra of the complexes **1**–**4** in CH_2Cl_2 solutions.

Table 2
Electrochemical data of the complexes **1**–**4**.

Complex	1st Reduction potential	2nd Reduction potential	3rd Reduction potential
1	−1.53	−1.94	–
2	−1.49	−1.82	−2.06
3	−1.80	−2.08	–
4	−1.72	−1.98	−2.17

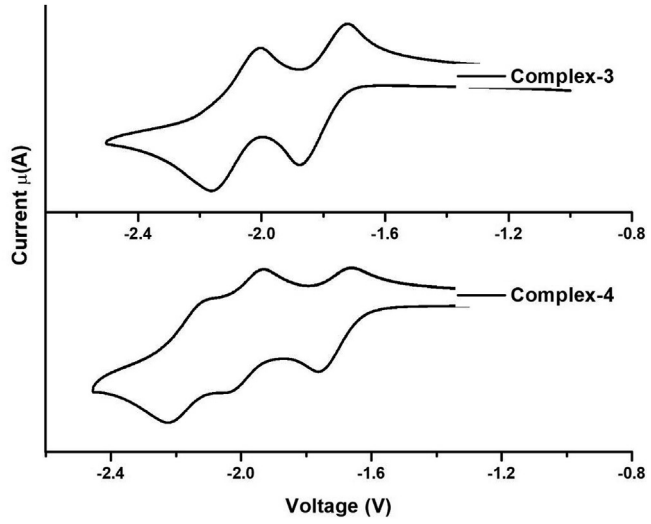

Fig. 6. Cyclic voltammogram of **3** and **4** with 0.1 M $Bu_4N(PF_6)$ in DME as the supporting electrolyte (scan rate 100 mV/s). Referenced relative to Fc/Fc^+ couple.

The photophysical properties of the ligands (**L1H$_2$** and **L2H$_3$**) and their boron complexes (**1**–**4**) in various solvents were recorded and the results are presented in Table 1. As expected the imine ligands showed very weak fluorescence in solution due to their intramolecular rotations or isomerisation upon irradiation [15,26,27,64]. After borylation significant change to the photophysical data has been observed. Absorption and emission spectra of the synthesized boron complexes in CH_2Cl_2 solution at a concentration of 35 μM are presented in Fig. 4. The difluoro- and diphenyl-boron complexes (**1**–**4**) have shown better molar absorption coefficients with bathochromic shift in comparison to the free ligands in the absorption spectrum (Fig. 4). The molar absorption coefficient of the boron complexes ranging from 16,500 $M^{-1}cm^{-1}$ to 39,900 $M^{-1}cm^{-1}$. Fig. 5 The molar absorption coefficient for the difluoro boron complexes (**1** & **2**) is much higher than their diphenyl boron complexes (**3** & **4**). The emission spectra recorded for complexes **1**–**4** showed moderate fluorescence (Table 1) upon boron chelation. Complexes **1**–**4** exhibit moderate quantum yields and did not show drastic emission changes with solvent polarity. This proves that interaction of boron complexes with solvent molecules in the excited state is less significant [26]. Complexes **3** & **4** exhibit large Stokes shift over complexes **1** & **2**, may be associated with irregular backbone of the molecules as a consequence of crowded environment. Such a crowding may enhance the intramolecular charge transfer process which leads to large Stokes shifts. Complexes **1** & **3** are weekly fluorescent in the solid state, however complexes **2** & **4** do not fluoresce in the solid state. The observed photophysical properties are comparable with literature reported compounds of similar type [38].

The electrochemical behaviours of complexes **1**–**4** were studied

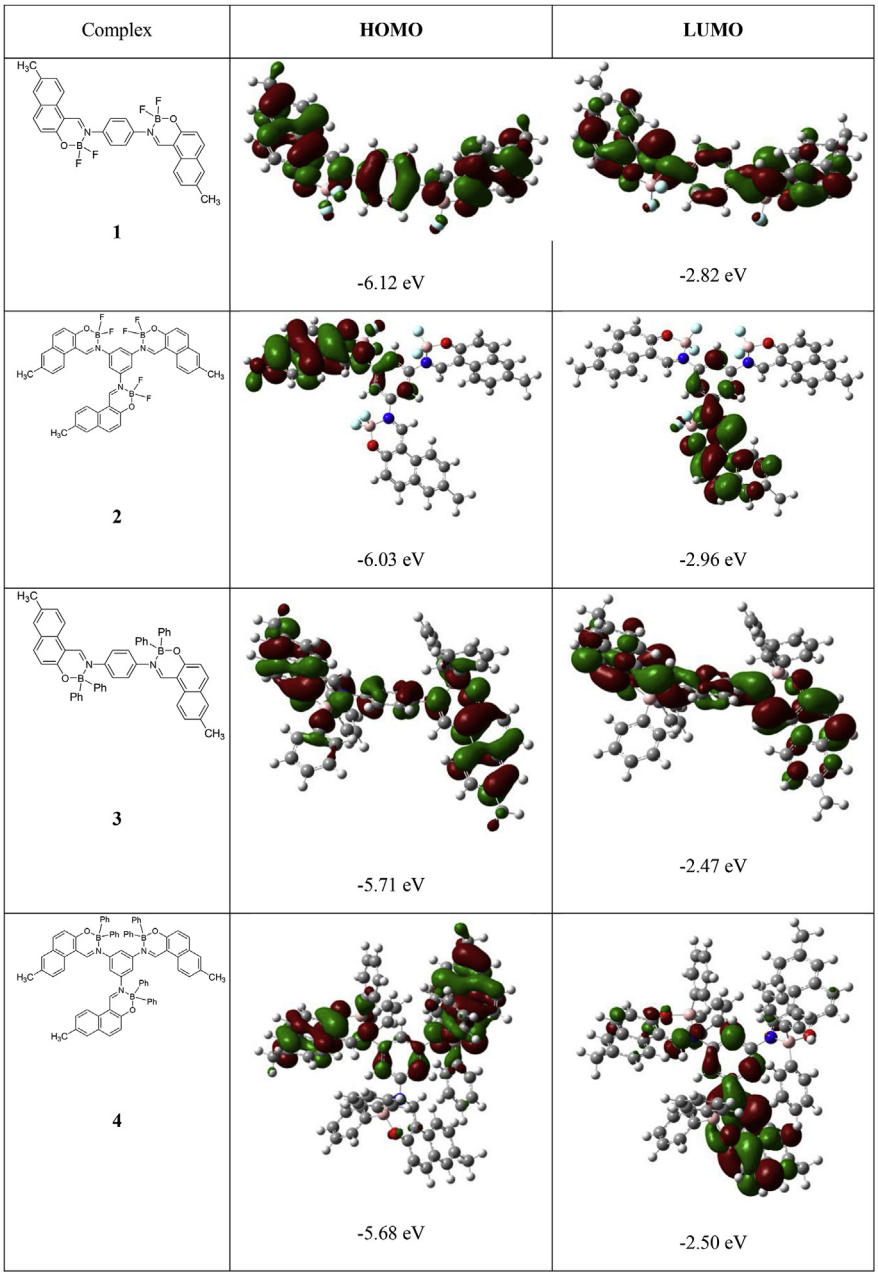

Fig. 7. Computed HOMOs and LUMOs for complexes **1**–**4**.

by cyclic voltammetry in DME solution. The di- and triboron complexes exhibit two and three electron reduction waves respectively (Table 2 & Fig. 6). Among the boron complexes studied (**1**–**4**); the first reduction potentials of difluoro boron complexes (**1** & **2**) are slightly less negative than those of diphenyl boron complexes (**3** & **4**). This may be due to the presence of electron withdrawing fluorine in complexes **1** & **2**.

In order to get more insights of absorption properties of complexes **1**–**4**, we carried out density functional theory (DFT) calculations. As shown in Fig. 7 (Table S2) the HOMOs and LUMOs of complexes **1** & **3** delocalized over naphthyl rings and the centre phenyl ring whereas in complexes **2** & **4** it is limited to one (or) two naphthyl units of the molecule. Diphenyl boron complexes **3** & **4** have shown higher HOMO energy level which is in line with the observed red shift in comparison to the difluoro substituted complexes **1** & **2**. Complexes **1** & **2** have slightly higher LUMO energy, a possible reason for the low electron reduction potentials observed in these complexes.

4. Conclusions

In conclusion, we have isolated and characterized four new tetra coordinate boron complexes. Two of them as difluoro boron complexes (**1** & **2**) and the other two as diphenyl boron complexes (**3** & **4**). The boron complexes **1**–**4** have shown better quantum yields over the ligands and better Stokes shift over BODIPY system. The increase of the number of boron *i.e.* from two boron (complex **1** or **3**) to three boron (complex **2** or **4**) center has considerable effect on the reduction potentials however does not have much influence on the photophysical properties.

Acknowledgements

The authors thank Science and Engineering Research Board (SERB) (EMR/2017/000620), New Delhi and Department of Atomic Energy (DAE) for financial support. RVRNC thank CSIR, New Delhi for research fellowship.

Appendix A. Supplementary data

Supplementary data to this article can be found online at https://doi.org/10.1016/j.jorganchem.2019.04.008.

References

[1] Y. Yan, Y.S. Zhao, Organic nanophotonics: from controllable assembly of functional molecules to low-dimensional materials with desired photonic properties, Chem. Soc. Rev. 43 (2014) 4325–4340.
[2] J. Liang, B.Z. Tang, B. Liu, Specific light-up bioprobes based on AIEgen conjugates, Chem. Soc. Rev. 44 (2015) 2798–2811.
[3] T. Weil, T. Vosch, J. Hofkens, K. Peneva, K. Müllen, The rylene colorant family—tailored nanoemitters for photonics research and applications, Angew. Chem. Int. Ed. 49 (2010) 9068–9093.
[4] H. Kobayashi, M. Ogawa, R. Alford, P.L. Choyke, Y. Urano, New strategies for fluorescent probe design in medical diagnostic imaging, Chem. Rev. 110 (2009) 2620–2640.
[5] L. Yuan, W. Lin, K. Zheng, L. He, W. Huang, Far-red to near infrared analyte-responsive fluorescent probes based on organic fluorophore platforms for fluorescence imaging, Chem. Soc. Rev. 42 (2013) 622–661.
[6] M.H. Lee, J.S. Kim, J.L. Sessler, Small molecule-based ratiometric fluorescence probes for cations, anions, and biomolecules, Chem. Soc. Rev. 44 (2015) 4185–4191.
[7] E. Climent, M. Biyikal, K. Gawlitza, T. Dropa, M. Urban, A.M. Costero, R. Martínez-Máñez, K. Rurack, A rapid and sensitive strip-based quick test for nerve agents tabun, sarin, and soman using BODIPY-modified silica materials, Chem. Eur J. 22 (2016) 11138–11142.
[8] Y. Lin, Y. Li, X. Zhan, Small molecule semiconductors for high-efficiency organic photovoltaics, Chem. Soc. Rev. 41 (2012) 4245–4272.
[9] A.W. Hains, Z. Liang, M.A. Woodhouse, B.A. Gregg, Molecular semiconductors in organic photovoltaic cells, Chem. Rev. 110 (2010) 6689–6735.
[10] A. Mishra, P. Bäuerle, Small molecule organic semiconductors on the move: promises for future solar energy technology, Angew. Chem. Int. Ed. 51 (2012) 2020–2067.
[11] M. Zhu, C. Yang, Blue fluorescent emitters: design tactics and applications in organic light-emitting diodes, Chem. Soc. Rev. 42 (2013) 4963–4976.
[12] X.-H. Zhu, J. Peng, Y. Cao, J. Roncali, Solution-processable single-material molecular emitters for organic light-emitting devices, Chem. Soc. Rev. 40 (2011) 3509–3524.
[13] N. Boens, V. Leen, W. Dehaen, Fluorescent indicators based on BODIPY, Chem. Soc. Rev. 41 (2012) 1130–1172.
[14] H. Lu, J. Mack, Y. Yang, Z. Shen, Structural modification strategies for the rational design of red/NIR region BODIPYs, Chem. Soc. Rev. 43 (2014) 4778–4823.
[15] D. Frath, J. Massue, G. Ulrich, R. Ziessel, Luminescent materials: locking π-conjugated and heterocyclic ligands with boron (III), Angew. Chem. Int. Ed. 53 (2014) 2290–2310.
[16] K.G. Thorat, G. Chowdhary, P. Isar, M. Ravikanth, Covalently linked meso-BODIPYnyl dithiahomoporphyrins: synthesis and properties, Eur. J. Org. Chem. 2018 (2018) 5389–5396.
[17] Y. Zhou, J.W. Kim, M.J. Kim, W.-J. Son, S.J. Han, H.N. Kim, S. Han, Y. Kim, C. Lee, S.-J. Kim, Novel bi-nuclear boron complex with pyrene ligand: red-light emitting as well as electron transporting material in organic light-emitting diodes, Org. Lett. 12 (2010) 1272–1275.
[18] Y. Zhou, Y. Xiao, S. Chi, X. Qian, Isomeric boron– fluorine complexes with donor– acceptor architecture: strong solid/liquid fluorescence and large Stokes shift, Org. Lett. 10 (2008) 633–636.
[19] J. Massue, D. Frath, G. Ulrich, P. Retailleau, R. Ziessel, Synthesis of luminescent 2-(2′-hydroxyphenyl) benzoxazole (HBO) borate complexes, Org. Lett. 14 (2011) 230–233.
[20] K. Benelhadj, J. Massue, G. Ulrich, 2, 4 and 2, 5-bis (benzooxazol-2′-yl) hydroquinone (DHBO) and their borate complexes: synthesis and optical properties, New J. Chem. 40 (2016) 5877–5884.
[21] Y. Kubota, T. Niwa, J. Jin, K. Funabiki, M. Matsui, Synthesis, absorption, and electrochemical properties of quinoid-type bisboron complexes with highly symmetrical structures, Org. Lett. 17 (2015) 3174–3177.
[22] M. Urban, K. Durka, P. Jankowski, J. Serwatowski, S. Lulinski, Highly fluorescent red-light emitting bis (boranils) based on naphthalene backbone, J. Org. Chem. 82 (2017) 8234–8241.
[23] D. Frath, P. Didier, Y. Mély, J. Massue, G. Ulrich, Vectorization and intracellular distribution of a two-photon-absorbing, near-infrared-emitting π-extended boranil dye, ChemPhotoChem 1 (2017) 109–112.
[24] D. Frath, S.b. Azizi, G. Ulrich, P. Retailleau, R. Ziessel, Facile synthesis of highly fluorescent boranil complexes, Org. Lett. 13 (2011) 3414–3417.
[25] D. Frath, S. Azizi, G. Ulrich, R. Ziessel, Chemistry on Boranils: an entry to functionalized fluorescent dyes, Org. Lett. 14 (2012) 4774–4777.
[26] J. Dobkowski, P. Wnuk, J. Buczyńska, M. Pszona, G. Orzanowska, D. Frath, G. Ulrich, J. Massue, S. Mosquera-Vázquez, E. Vauthey, Substituent and solvent effects on the excited state deactivation channels in anils and boranils, Chem. Eur J. 21 (2015) 1312–1327.
[27] G. Wesela-Bauman, M. Urban, S. Luliński, J. Serwatowski, K. Woźniak, Tuning of the colour and chemical stability of model boranils: a strong effect of structural modifications, Org. Biomol. Chem. 13 (2015) 3268–3279.
[28] P. Zhang, W. Liu, G. Niu, H. Xiao, M. Wang, J. Ge, J. Wu, H. Zhang, Y. Li, P. Wang, Coumarin-based boron complexes with aggregation-induced emission, J. Org. Chem. 82 (2017) 3456–3462.
[29] J.F. Araneda, W.E. Piers, B. Heyne, M. Parvez, R. McDonald, High Stokes shift anilido-pyridine boron difluoride dyes, Angew. Chem. Int. Ed. 50 (2011) 12214–12217.
[30] D. Curiel, M. Más-Montoya, L. Usea, A. Espinosa, R.A. Orenes, P. Molina, Indolocarbazole-based ligands for ladder-type four-coordinate boron complexes, Org. Lett. 14 (2012) 3360–3363.
[31] G.M. Fischer, E. Daltrozzo, A. Zumbusch, Selective NIR chromophores: bis (pyrrolopyrrole) cyanines, Angew. Chem. Int. Ed. 50 (2011) 1406–1409.
[32] W. Li, W. Lin, J. Wang, X. Guan, Phenanthro [9, 10-d] imidazole-quinoline boron difluoride dyes with solid-state red fluorescence, Org. Lett. 15 (2013) 1768–1771.
[33] D. Zhao, G. Li, D. Wu, X. Qin, P. Neuhaus, Y. Cheng, S. Yang, Z. Lu, X. Pu, C. Long, Regiospecific N-heteroarylation of amidines for full-color-tunable boron difluoride dyes with mechanochromic luminescence, Angew. Chem. Int. Ed. 52 (2013) 13676–13680.
[34] N. Gao, C. Cheng, C. Yu, E. Hao, S. Wang, J. Wang, Y. Wei, X. Mu, L. Jiao, Facile synthesis of highly fluorescent BF_2 complexes bearing isoindolin-1-one ligand, Dalton Trans. 43 (2014) 7121–7127.
[35] J. Yoshino, N. Kano, T. Kawashima, Synthesis of organoboron compounds bearing an azo group and substituent effects on their structures and photoisomerization, Tetrahedron 64 (2008) 7774–7781.
[36] M.S. Baranov, K.A. Lukyanov, A.O. Borissova, J. Shamir, D. Kosenkov, L.V. Slipchenko, L.M. Tolbert, I.V. Yampolsky, K.M. Solntsev, Conformationally locked chromophores as models of excited-state proton transfer in fluorescent proteins, J. Am. Chem. Soc. 134 (2012) 6025–6032.
[37] V.F. Pais, M.M. Alcaide, R. López-Rodríguez, D. Collado, F. Nájera, E. Pérez-Inestrosa, E. Álvarez, J.M. Lassaletta, R. Fernández, A. Ros, Strongly emissive and photostable four-coordinate organoboron N, C chelates and their use in fluorescence microscopy, Chem. Eur J. 21 (2015) 15369–15376.
[38] D. Frath, K. Benelhadj, M. Munch, J. Massue, G. Ulrich, Polyanils and polyboranils: synthesis, optical properties, and aggregation-induced emission,

J. Org. Chem. 81 (2016) 9658–9668.
[39] Y. Zhou, J.W. Kim, R. Nandhakumar, M.J. Kim, E. Cho, Y.S. Kim, Y.H. Jang, C. Lee, S. Han, K.M. Kim, Novel binaphthyl-containing bi-nuclear boron complex with low concentration quenching effect for efficient organic light-emitting diodes, Chem. Commun. 46 (2010) 6512–6514.
[40] P. Gong, H. Yang, J. Sun, Z. Zhang, J. Sun, P. Xue, R. Lu, Salicylaldimine difluoroboron complexes containing tert-butyl groups: nontraditional π-gelator and piezofluorochromic compounds, J. Mater. Chem. C 3 (2015) 10302–10308.
[41] J.A. Riddle, S.P. Lathrop, J.C. Bollinger, D. Lee, Schiff base route to stackable pseudo-triphenylenes: stereoelectronic control of assembly and luminescence, J. Am. Chem. Soc. 128 (2006) 10986–10987.
[42] Z. Zhang, H. Bi, Y. Zhang, D. Yao, H. Gao, Y. Fan, H. Zhang, Y. Wang, Y. Wang, Z. Chen, D. Ma, Luminescent boron-contained ladder-type π-conjugated compounds, Inorg. Chem. 48 (2009) 7230–7236.
[43] D. Li, Y. Yuan, H. Bi, D. Yao, X. Zhao, W. Tian, Y. Wang, H. Zhang, Boron-bridged π-conjugated ladders as efficient electron-transporting emitters, Inorg. Chem. 50 (2011) 4825–4831.
[44] E. Hadjoudis, I.M. Mavridis, Photochromism and thermochromism of Schiff bases in the solid state: structural aspects, Chem. Soc. Rev. 33 (2004) 579–588.
[45] M. Ziółek, B. Cohen, X. Yang, L. Sun, M. Paulose, O.K. Varghese, C.A. Grimes, A. Douhal, Femtosecond to millisecond studies of electron transfer processes in a donor–(π-spacer)–acceptor series of organic dyes for solar cells interacting with titania nanoparticles and ordered nanotube array films, Phys. Chem. Chem. Phys. 14 (2012) 2816–2831.
[46] T. Sekikawa, O. Schalk, G. Wu, A.E. Boguslavskiy, A. Stolow, Initial processes of proton transfer in salicylideneaniline studied by time-resolved photoelectron spectroscopy, J. Phys. Chem. A 117 (2013) 2971–2979.
[47] L. Spörkel, G. Cui, W. Thiel, Photodynamics of schiff base salicylideneaniline: trajectory surface-hopping simulations, J. Phys. Chem. A 117 (2013) 4574–4583.
[48] M. Ziółek, G. Burdziński, A. Douhal, Long-living structures of photochromic salicylaldehyde azine: polarity and viscosity effects from nanoseconds to hours, Photochem. Photobiol. Sci. 11 (2012) 1389–1400.
[49] M. Ziółek, C. Martín, M.T. Navarro, H. Garcia, A. Douhal, Confined photodynamics of an organic dye for solar cells encapsulated in titanium-doped mesoporous molecular materials, J. Phys. Chem. C 115 (2011) 8858–8867.
[50] A. Grabowska, K. Kownacki, J. Karpiuk, S. Dobrin, Photochromism and proton transfer reaction cycle of new internally H-bonded Schiff bases, Chem. Phys. Lett. 267 (1997) 132–140.
[51] K. Kownacki, A. Mordzinski, R. Wilbrandt, A. Grabowska, Laser-induced absorption and fluorescence studies of photochromic Schiff bases, Chem. Phys. Lett. 227 (1994) 270–276.
[52] N. Otsubo, C. Okabe, H. Mori, K. Sakota, K. Amimoto, T. Kawato, H. Sekiya, Excited-state intramolecular proton transfer in photochromic jet-cooled N-salicylideneaniline, J. Photochem. Photobiol., A 154 (2002) 33–39.
[53] W.M. Fabian, L. Antonov, D. Nedeltcheva, F.S. Kamounah, P.J. Taylor, Tautomerism in hydroxynaphthaldehyde anils and azo analogues: a combined experimental and computational study, J. Phys. Chem. A 108 (2004) 7603–7612.
[54] K. Dhanunjayarao, V. Mukundam, M. Ramesh, K. Venkatasubbaiah, Synthesis and optical properties of salicylaldimine-based diboron complexes, Eur. J. Inorg. Chem. 2014 (2014) 539–545.
[55] K. Dhanunjayarao, V. Mukundam, R.V.R.N. Chinta, K. Venkatasubbaiah, Synthesis of highly fluorescent imidazole based diboron complex, J. Organomet. Chem. 865 (2018) 234–238.
[56] K. Niimi, M.J. Kang, E. Miyazaki, I. Osaka, K. Takimiya, General synthesis of dinaphtho [2, 3-b: 2′, 3′-f] thieno [3, 2-b] thiophene (DNTT) derivatives, Org. Lett. 13 (2011) 3430–3433.
[57] B.S. Kumar, K. Ravi, A.K. Verma, K. Fatima, M. Hasanain, A. Singh, J. Sarkar, S. Luqman, D. Chanda, A.S. Negi, Synthesis of pharmacologically important naphthoquinones and anticancer activity of 2-benzyllawsone through DNA topoisomerase-II inhibition, Bioorg. Med. Chem. 25 (2017) 1364–1373.
[58] G.M. Sheldrick, SHELXT–Integrated space-group and crystal-structure determination, Acta Crystallogr. A: Found. Adv. 71 (2015) 3–8.
[59] Hexyl-group was introduced on the naphthyl in order to increase the solubility; Without "hexyl" the Products Showed Limited Solubility.
[60] This is presumably caused by the fast ring-flipping associated with the complex in solution at room temperature.
[61] A. Moeller, P. Bleckenwegner, U. Monkowius, F. Mohr, Gold(I)alkynyl complexes decorated with chromophores: structural, photophysical and computational studies, J. Organomet. Chem. 813 (2016) 1–6.
[62] H. Mtiraoui, R. Gharbi, M. Msaddek, Y. Bretonniere, C. Andraud, P.-Y. Renard, C. Sabot, Solution and solid-state fluorescence of 2-(2'-hydroxyphenyl)-1,5-benzodiazepin-2-one (HBD) borate complexes, RSC Adv. 6 (2016) 86352–86360.
[63] J. Shanmugapriya, K. Rajaguru, G. Sivaraman, S. Muthusubramanian, N. Bhuvanesh, Boranil dye based "turn-on" fluorescent probes for detection of hydrogen peroxide and their cell imaging application, RSC Adv. 6 (2016) 85838–85843.
[64] A.M. Grabarz, A.l.D. Laurent, B. Jedrzejewska, A. Zakrzewska, D. Jacquemin, B. Osmiałowski, The influence of the π-conjugated spacer on photophysical properties of difluoroboranyls derived from amides carrying a donor group, J. Org. Chem. 81 (2016) 2280–2292.